PRIFYSGOL glyndŵr UNIVERSITY

Glyndŵr University Research Online

Conference Paper

Temperature gradient improvement of power semiconductor modules cooled using forced air heat sink

Sharp, A., Monir, S., Vagapov. Y. and Day, R.J.

This is a paper presented at the Proc. XIV International Symposium on Industrial Electronics and Applications INDEL-2022, Banja Luka, Bosnia and Herzegovina, 9-11 Nov.

Copyright of the author(s). Reproduced here with their permission and the permission of the conference organisers.

Recommended citation:

Sharp, A., Monir, S., Vagapov. Y. and Day, R.J. (2022), 'Temperature gradient improvement of power semiconductor modules cooled using forced air heat sink.' In: Proc. XIV International Symposium on Industrial Electronics and Applications INDEL-2022, Banja Luka, Bosnia and Herzegovina, 9-11 Nov. 2022, pp. 1-5. doi: 10.1109/INDEL55690.2022.9965507.
Available at: https://ieeexplore.ieee.org/document/9965507

Temperature Gradient Improvement of Power Semiconductor Modules Cooled Using Forced Air Heat Sink

Andrew Sharp
Faculty of Art, Science and Technology
Glyndwr University
Wrexham, UK

Shafiul Monir
Faculty of Art, Science and Technology
Glyndwr University
Wrexham, UK

Yuriy Vagapov
Faculty of Art, Science and Technology
Glyndwr University
Wrexham, UK

Richard J. Day
Faculty of Art, Science and Technology
Glyndwr University
Wrexham, UK

***Abstract*—This paper discusses the improvement of operational reliability and lifetime of power electronic modules due to the reduction of the temperature gradient in the semiconductor structures. High temperature gradient in the power electronic modules having a large area of the semiconductor structure is a more affecting issue than the junction temperature. The improvement in the temperature gradient is achieved by varying/degrading the thermal resistance along the heat sink length. A conventional cooling system for three semiconductor modules based on a forced air heat sink was modelled and analysed to derive a reduction rate of the appropriate thermal resistances. Implementation of the forced air heat sink having non-uniformed thermal resistances along the heat sink length ensures the uniform temperature distribution across the power semiconductors and, therefore, the improved thermal gradient.**

Keywords—temperature gradient, power electronic module, IGBT, power semiconductor reliability, forced air heat sink

I. Introduction

Electric drive systems are a rapidly growing area of industrial applications consuming approximately half of the electrical energy generated in the world [1]. An important component of the electric drive is the power electronic inverter, which provides the appropriate operation of an electric motor according to an intended control algorithm. The inverter as the most electrically and thermally loaded element of the drive circuit mainly determines the safety and reliability of the system processing [2]. Yang *et al.* [3] reported that about 31% of total component failures in power electronic devices occur due to the failure of converter power semiconductors.

The thermal stress of the power semiconductors composing electric drive inverters depends on two major factors. The first factor is the temperature of the ambient affecting the thermal condition of the junction – the ambient temperature value can be high, particularly in high-power density applications. The second factor is the power loss produced in the junction due to the load profile. Both factors have a significant influence on the temperature of the semiconductors and are the main causes of the component overheating [4].

The most common approach to power semiconductor heat management is a heat sink providing the transfer of heat power from the junction to the environment. Natural and forced air-cooled heat sinks are considered effective and inexpensive solutions, widely used in industrial installations. Many electric/electronic manufacturers offer a large variety of air-cooled heat sinks for various power electronic applications, where three (or six) semiconductor modules are usually installed on the top of the heat sink alongside the rectangular surface. The number of semiconductor modules depends on the module internal circuitry, which usually represents one or two semiconductor switches to build a six-switch inverter.

In case of forced air cooling, the fan is located at one side of the heat sink to provide airflow through the fins. Such a heat sink configuration causes the temperature difference alongside the heat sink length. It means that the temperatures of the semiconductor modules are different. The device installed close to the airflow inlet has the lowest temperature and is thermally underloaded, while the temperature of the device at the opposite end is the highest. This semiconductor module has the highest thermal load, and its condition determines the reliability of the entire system.

Apart from the variation in the thermal loads, the temperature difference occurred in a forced air-cooled heat sink produces a high temperature gradient across the heat sink surface and, therefore, across the semiconductor module surface. The modern, high power semiconductor modules have a large surface area of the semiconductor structure. For example, the total surface area of the transistors and diodes in the IGBT module CM400T-24S [5] is about 50 cm^2 (approximal dimensions of the semiconductor structure in the module CM400T-24S are shown in Fig. 1; Fig. 2 illustrates a cross-sectional view of a typical IGBT module installed on the heat sink top surface). A high temperature gradient creates mechanical stress in the structure of the semiconductor and it has a negative impact on the reliability of operation and the lifetime of the module. For the power electronic modules having a large area of the semiconductor structure, the temperature gradient becomes a more important reliability issue in comparison to the junction temperature [6],[7].

There are a few methods for reducing the temperature difference between the power semiconductors and, therefore, improving the temperature gradient. An advanced method called active thermal control focuses on the redistribution or/and adjustment of power loss in semiconductor junctions to uniform the temperature [8]-[10]. This method does not require hardware modification but demonstrates reduced operational efficiency and increases the total amount of power loss. Another approach is related to the application of the variable thermal resistance alongside the heat sink [11],[12]. This method

978-1-6654-7187-9/22/$31.00 ©2022 IEEE

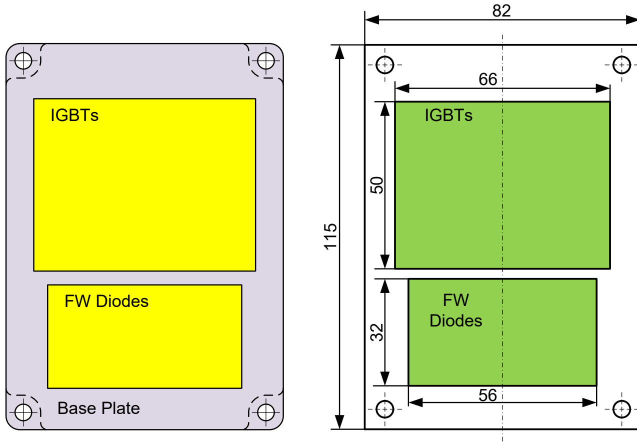

Fig. 1. Area of the semiconductor structure of the IGBT module CM400T-24S [5] (approx. 50 cm^2).

requires modification of the heat sink to ensure the uniform temperature of the power electronic modules due to the non-uniform thermal resistance distribution. The power converter cooled using this approach has the temperature of all semiconductors similar to the hottest device but a negligible temperature gradient.

This paper analyses a modification of a standard heat sink to implement variable thermal resistances along the heat sink length. The thermal resistances are varied in a way to provide the same temperature in the semiconductor modules and to reduce the thermal gradient. In order to increase/adjust the appropriate thermal resistance, the corresponding area of the heat sink is mechanically modified to degrade the heat transfer conditions.

II. Forced Air Heat Sink Cooling System

Fig. 3 shows a schematic diagram of the conventional forced air heat sink configuration having three power semiconductor modules (IGBT) installed on the top in a row. The fan blowing air into the heat sink fin area is located at the inlet of the cooling system. The heat sink is virtually divided into 3 sections (A, B, and C). Each section has a thermal resistance (heat sink – ambient) and there are two thermal resistances between sections A/B and B/C. If the thermal resistances of each section are the same, then the temperature on the top surface of the heat sink is increased from section A to section B, producing the temperature gradient.

The thermal equivalent circuit of the analysed cooling system is shown in Fig. 4. The circuit was derived from the approach presented and discussed in [9],[11],[13],[14]. According to the equivalent circuit, it can be seen that the temperature of each section of the heatsink T_A, T_B, and T_C are defined as follows:

$$\begin{cases} T_A = T_{AIR} + \tau_1 \\ T_B = T_{AIR} + \tau_A + \tau_2 \\ T_C = T_{AIR} + \tau_A + \tau_B + \tau_3 \end{cases} \quad (1)$$

where T_{AIR} is the temperature of ambient air; τ_1, τ_2, and τ_3 are temperature drops across thermal resistances R_{T1}, R_{T2}, and R_{T3}; τ_A and τ_B are the temperatures of the thermal sources reflecting the air temperature increase alongside the heatsink length.

It is assumed that the temperature of the thermal sources in the thermal equivalent circuit is proportional to the temperature drop across the thermal resistances R_{T1} or R_{T2}.

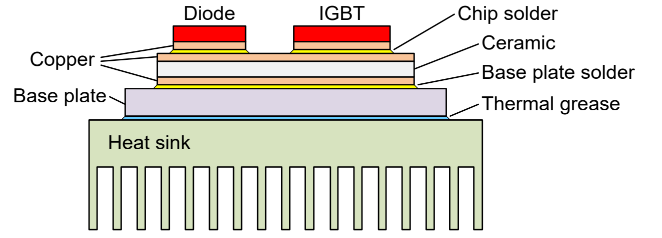

Fig. 2. Cross-sectional view of a typical IGBT module installed on the heat sink top surface.

This assumption introduces the coefficient k_τ which is providing the link between temperature drop across a heat sink section thermal resistor and corresponding source temperature and is expressed as a ratio $k_\tau = \tau_A/\tau_1 = \tau_B/\tau_2$. In general, the coefficient depends on the airflow rate through the heat sink and the thermal capacitance of the air. Hence, the temperatures of the circuit thermal sources are determined using the following equations:

$$\begin{cases} \tau_A = k_\tau \left(T_A - T_{AIR}\right) = k_\tau \tau_1 \\ \tau_B = k_\tau \left(T_B - \tau_A - T_{AIR}\right) = k_\tau \tau_2 \end{cases} \quad (2)$$

The temperatures of the IGBT modules are shown as junctions in the thermal equivalent circuit. Therefore, resolving the junctions problem in terms of the incoming and leaving power flows, the power loss generated by the IGBT modules P_1, P_2, and P_3 can be expressed as follows:

$$\begin{cases} P_1 = P_{C1} + P_{R1} - P_{R12} \\ P_2 = P_{R12} + P_{C2} + P_{R2} - P_{R23} \\ P_3 = P_{R23} + P_{C3} + P_{R3} \end{cases} \quad (3)$$

where P_1, P_2, and P_3 are power loss in the IGBT modules A, B, and C respectively; P_{R12} is the power flow from IGBT module B to IGBT module A; P_{R23} is the power flow from IGBT module C to IGBT module B; P_{R1}, P_{R2}, and P_{R3} are power flow through thermal resistors R_{T1}, R_{T2}, and R_{T3}; P_{C1}, P_{C2}, and P_{C3} are power flow through thermal heat capacitors C_1, C_2, and C_3.

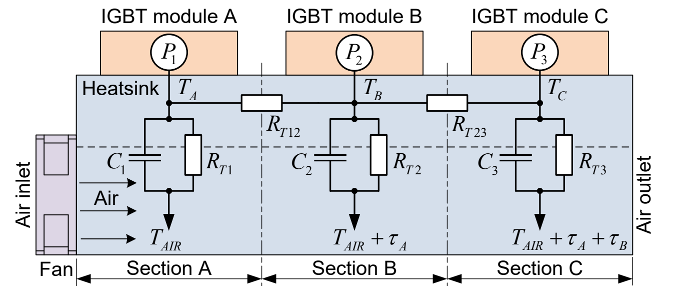

Fig. 3. Schematic diagram of the three-mass thermal model of the cooling system.

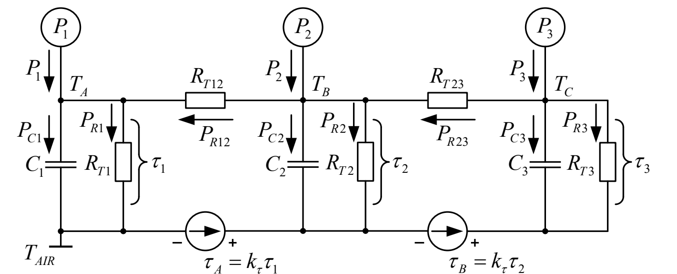
Fig. 4. Thermal equivalent circuit of the cooling system.

The heat sink is considered as a combination of three sections A, B, and C where each section is represented by the thermal heat capacity. Therefore, the power flows P_{C1}, P_{C2}, and P_{C3} through the thermal capacitors are defined as:

$$P_{C1} = C_1 \frac{d\tau_1}{dt};\; P_{C2} = C_2 \frac{d\tau_2}{dt};\; P_{C3} = C_3 \frac{d\tau_3}{dt} \quad (4)$$

The thermal heat capacitors are calculated using the specific thermal capacity of the heat sink material and the appropriate mass of the heat sink section:

$$C_1 = c_h \times m_A;\; C_2 = c_h \times m_B;\; C_3 = c_h \times m_C \quad (5)$$

where c_h is the specific heat capacity of the heat sink material (aluminium); m_A, m_B, and m_C are the masses of the corresponding sections A, B, and C of the heat sink.

Power flows between the heat sink sections P_{R12} and P_{R23} are as follows:

$$\begin{cases} P_{R12} = \dfrac{T_B - T_A}{R_{T12}} = \dfrac{\tau_A + \tau_2 - \tau_1}{R_{T12}} \\ P_{R23} = \dfrac{T_C - T_B}{R_{T23}} = \dfrac{\tau_B + \tau_3 - \tau_2}{R_{T23}} \end{cases} \quad (6)$$

where R_{T12} is the thermal resistance between heatsink sections A and B; R_{T23} is the thermal resistance between heatsink sections B and C.

Substituting (4) and (5) into (3):

$$\begin{cases} P_1 = C_1 \dfrac{d\tau_1}{dt} + \dfrac{\tau_1}{R_{T1}} - \dfrac{\tau_2 + k_\tau \tau_1 - \tau_1}{R_{T12}} \\ P_2 = C_2 \dfrac{d\tau_2}{dt} + \dfrac{\tau_2}{R_{T2}} + \dfrac{\tau_2 + k_\tau \tau_1 - \tau_1}{R_{T12}} - \dfrac{\tau_3 + k_\tau \tau_2 - \tau_2}{R_{T23}} \\ P_3 = C_3 \dfrac{d\tau_3}{dt} + \dfrac{\tau_3}{R_{T3}} + \dfrac{\tau_3 + k_\tau \tau_2 - \tau_2}{R_{T23}} \end{cases} \quad (7)$$

Rearranging (7) for Simulink modelling and simulation:

$$\begin{cases} P_1 + \dfrac{\tau_1 (k_\tau - 1) + \tau_2}{R_{T12}} = \dfrac{\tau_1 (sC_1 R_{T1} + 1)}{R_{T1}} \\ P_2 - \dfrac{\tau_1 (k_\tau - 1) + \tau_2}{R_{T12}} + \dfrac{\tau_2 (k_\tau - 1) + \tau_3}{R_{T23}} = \dfrac{\tau_2 (sC_2 R_{T2} + 1)}{R_{T2}} \\ P_3 - \dfrac{\tau_2 (k_\tau - 1) + \tau_3}{R_{T23}} = \dfrac{\tau_3 (sC_3 R_{T3} + 1)}{R_{T3}} \end{cases} \quad (8)$$

This set of equations has been used to build the Simulink model of the thermal model of the three-phase inverter cooling system. Fig. 5 shows the block diagram of the 3-mass thermal model developed according to the set of equations (8).

The model was simulated using MATLAB Simulink software environment. The heat sink selected for the simulation is the standard heat sink I71 [15] having the dimensions W130.4mm × H57mm × L310mm. It was assumed that the simulation model has three IGBT modules CM400T-24S1 [5] installed on the top of the heat sink. The thermal resistances (for section A, B, and C) of the equivalent circuit were derived using both the heat sink geometry and airflow speed (5 m/s) where $R_{T1} = R_{T2} = R_{T3} = 0.32$°C/W, $R_{T12} = R_{T23} = 0.25$°C/W. The coefficient $k_\tau = 0.18$, the thermal capacity of each heat sink section $C_1 = C_2 = C_3 = 100$ J/°C, and the room temperature is 25°C. The simulation was conducted under condition: the

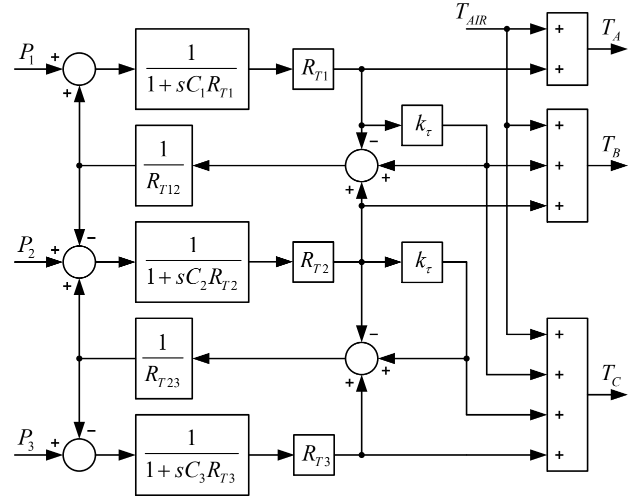

Fig. 5. Simulink model of the thermal equivalent circuit.

power loss generated in each IGBT module is 100W per module.

The simulation result in Fig. 6 demonstrates a difference in temperature (approx. 3°C at the steady-state condition) between the IGBT modules. Though the absolute values do

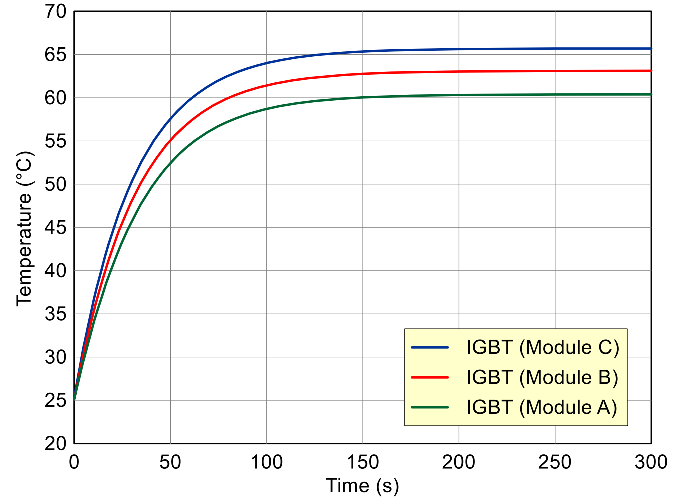

Fig. 6. The temperature transient of IGBT modules.

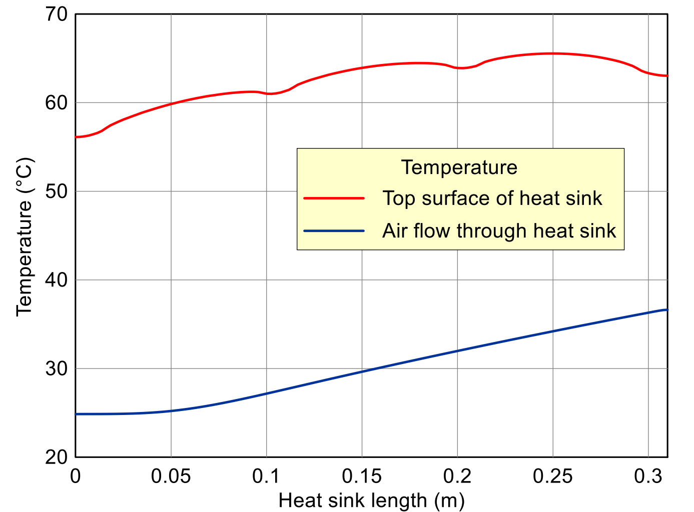

Fig. 7. The temperature along the middle line on the top surface of the heat sink (red) and the temperature of the airflow through the heat sink (blue) versus the heat sink length (310cm).

not exceed the rated module temperature, the different temperatures indicate the thermal gradient occurring due to uniform thermal resistances along the heat sink. Therefore, the temperature difference is assumed to be an indirect indicator of the thermal gradient in the semiconductor structure. The discussed simulation model (Fig. 5) is a fast approach to estimating the gradient of temperature across the power electronic modules.

However, a more detailed numerical simulation can provide the results with better accuracy. For example, Fig. 7 shows the results obtained from the simulation of the same cooling system conducted using ANSYS software. The red curve in Fig. 7 shows the temperature in the middle line on the top surface of the heat sink, whereas the blue curve is the air temperature in the middle of the fin area of the heat sink. It can be seen that there is a temperature gradient affecting the IGBT modules. What is more, the IGBT module A located by the air inlet and having the lowest temperature is the semiconductor device most affected by the temperature gradient in comparison to other modules.

III. Temperature Gradient Improvement

In terms of steady-state operation, the set of equations (7) can be reduced to the following expression, where the components providing the circuit dynamic performance are omitted:

$$\begin{cases} P_1 = \dfrac{\tau_1}{R_{T1}} - \dfrac{\tau_1(k_\tau - 1) + \tau_2}{R_{T12}} \\ P_2 = \dfrac{\tau_2}{R_{T2}} + \dfrac{\tau_1(k_\tau - 1) + \tau_2}{R_{T12}} - \dfrac{\tau_2(k_\tau - 1) + \tau_3}{R_{T23}} \\ P_3 = \dfrac{\tau_3}{R_{T3}} + \dfrac{\tau_2(k_\tau - 1) + \tau_3}{R_{T23}} \end{cases} \tag{9}$$

The power loss generated in IGBTs operating under conventional balanced mode is the same in each power semiconductor module. Therefore, for further analysis, it can be replaced as $P = P_1 = P_2 = P_3$.

The best improvement of the temperature gradient can be obtained if the temperature of each semiconductor module is the same. If the temperature of power semiconductors A, B, and C are the same ($T_A = T_B = T_C$) then the power flows between the heat sink sections are neglected ($P_{R12} = P_{R23} = \infty$). Therefore, (9) is rearranged to obtain the formula as follows:

$$\frac{\tau_1}{R_{T1}} = \frac{\tau_2}{R_{T2}} = \frac{\tau_3}{R_{T3}} \tag{10}$$

Substituting (1) into (10):

$$\frac{\tau_1}{R_{T1}} = \frac{\tau_1 - \tau_A}{R_{T2}} = \frac{\tau_1 - \tau_A - \tau_B}{R_{T3}} \tag{11}$$

and (2) into (11)

$$\frac{\tau_1}{R_{T1}} = \frac{\tau_1 - k_\tau \tau_1}{R_{T2}} = \frac{\tau_1 - k_\tau \tau_1 - k_\tau(\tau_1 - k_\tau \tau_1)}{R_{T3}} \tag{12}$$

Hence,

$$\frac{1}{R_{T1}} = \frac{1 - k_\tau}{R_{T2}} = \frac{(1 - k_\tau)^2}{R_{T3}} \tag{13}$$

If the thermal resistor R_{T3} is considered as the base resistor representing 100% then the other thermal resistors R_{T1} and R_{T2} can be calculated in respect to R_{T3} as follows:

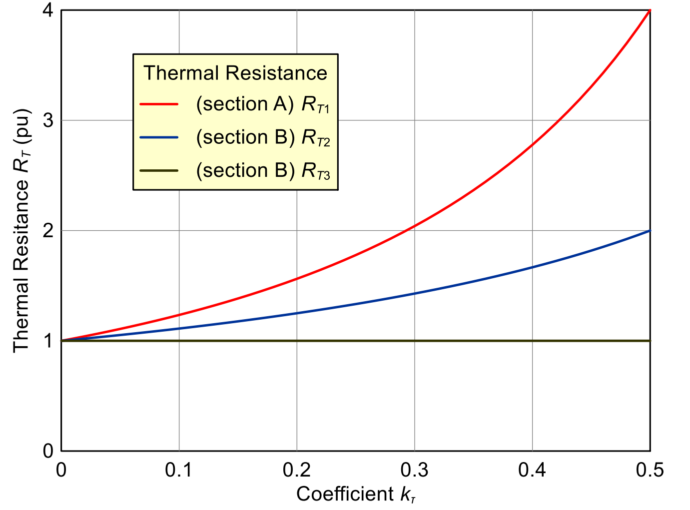

Fig. 8. Thermal resistances of the heat sink sections R_{T1}, R_{T2} and R_{T3} (in pu) versus the coefficient k_τ providing the link between temperature drop across a thermal resistor and corresponding source temperature.

$$R_{T2} = \frac{R_{T3}}{1 - k_\tau}\,;\, R_{T1} = \frac{R_{T3}}{(1 - k_\tau)^2} \tag{14}$$

This equation shows the increase rate of the thermal resistances R_{T1} and R_{T2} relatively to the thermal resistor R_{T3}. If the thermal resistance R_{T3} is known, (14) provides an understating of how the heat sink sections A and B should be modified (or designed) to ensure the required increase. Fig. 8 demonstrates the curves of the thermal resistances R_{T1}, R_{T2} and R_{T3} (in per unit) versus the coefficient k_τ.

The value of thermal resistance in the required heat sink sections can be increased according to (14) by reducing both the surface area and the air speed to ensure the improvement of the temperature gradient. Fig. 9 demonstrates an example of the temperature gradient improvement on the surface area of the heat sink obtained from the ANSYS simulation. The temperature distribution of the conventional cooling system analysed in the previous section is shown in Fig. 9a. It can be seen that the surface temperature of the heat sink having uniform thermal resistances has a significant gradient, which affects the IGBT modules installed on the top. Fig. 9b shows the temperature distribution of the heat sink where the thermal resistances in sections A and B have been degraded (increased) using the reduction of the airspeed through the fin area as proposed in [12]. Though the absolute temperature of the power semiconductor modules A and B are increased, the temperature gradient is improved

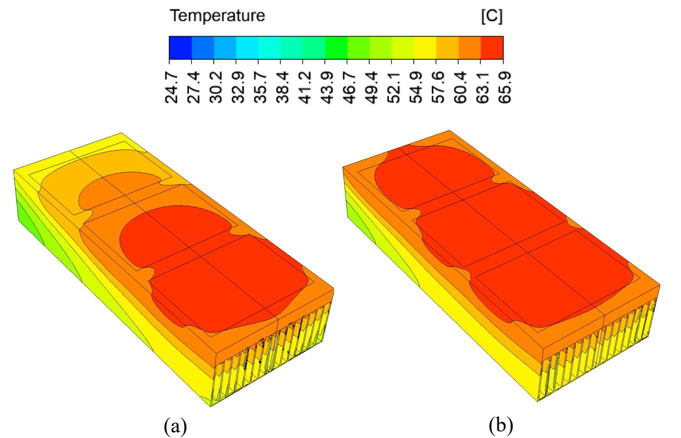

Fig. 9. Temperature distribution: (a) conventional cooling system having uniformed thermal resistances; (b) non-uniformed thermal resistances.

in comparison to the conventional heat sink configuration (Fig. 9a). It means that the applied measures reduced the thermo-mechanical stress in the semiconductor structures.

IV. Conclusion

For power electronic modules having a large area of the semiconductor structure, the high temperature gradient causes the thermo-mechanical stress in the semiconductor and, therefore, affects the operation reliability and the lifetime of the device. It is admitted that the temperature gradient has a more negative impact on the semiconductor condition than the high junction temperature.

This paper provides a discussion on the improvement of temperature gradients in forced air-cooled heat sinks where power semiconductor modules are installed at the top in a row. The disadvantage of the conventional cooling heat sink configuration is that the length of the thermal gradient along the heat sink occurs as a result of the gradual increase in the temperature of the airflow through the fin area. The improvement in the thermal gradient can be achieved by varying/degrading the thermal resistance along the heat sink length.

Following the thermal model described in the paper, the heat sink is divided into three sections, where each section is represented by a thermal resistance (heat sink – ambient). The increase (degradation) of the thermal resistances of the sections located by the air inlet ensures a uniform distribution of the temperature along the heat sink length. The model was analysed to derive the thermal resistance increase rate required for the gradient improvement. The analysis is underpinned by the results obtained from simulations conducted in MATLAB Simulink and ANSYS.

References

[1] A. Anuchin and Y. Vagapov, "Instructional laboratory for practical investigation of electric drive control," *IET Circuits, Devices and Systems*, vol. 11, no. 4, pp. 344-351, 2017, doi: 10.1049/iet-cds.2016.0400

[2] A. Abuelnaga, M. Narimani, and A.S. Bahman, "Power electronic converter reliability and prognosis review focusing on power switch module failures," *Journal of Power Electronics*, vol. 21, no. 6, pp. 865-880, June 2021, doi: 10.1007/s43236-021-00228-6

[3] S. Yang, A. Bryant, P. Mawby, D. Xiang, L. Ran, and P. Tavner, "An industry-based survey of reliability in power electronic converters," *IEEE Trans. on Industry Applications*, vol. 47, no. 3, pp. 1441-1451, May-June 2011, doi: 10.1109/TIA.2011.2124436

[4] S. Kascak and P. Resutik, "Method for estimation of power losses and thermal distribution in power converters," *Electrical Engineering*, vol. 104, no. 1, pp. 179-190, 2022, doi: 10.1007/s00202-021-01303-8

[5] Mitsubishi Electronics, "IGBT Moudule S1 series CM400ST-24S1," [Online]. Available: https://www.mitsubishielectric.com/semiconductors/content/product/powermodule/igbt/s1_series/cm400st-24s1_e.pdf

[6] H. Wu, C. Ye, Y. Zhang, F. Hou, and J. Nie, "Research on lifetime distribution and reliability of IGBT module based on accelerated life test and K-S test," *Int. Journal of Engineering Systems Modelling and Simulation*, vol. 11, no. 1, pp. 1-10, 2019, doi: 10.1504/IJESMS.2019.098903

[7] B. Gao, F. Yang, M. Chen, L.i. Ran, I. Ullah, S. Xu, and P. Mawby, "A temperature gradient-based potential defects identification method for IGBT module," *IEEE Trans. on Power Electronics*, vol. 32, no. 3, pp. 2227-2242, Mar. 2017, doi: 10.1109/TPEL.2016.2565701

[8] A. Anuchin, V. Podzorova, V. Popova, I. Gulyaev, F. Briz, and Y. Vagapov, "Model predictive torque control of a switched reluctance drive with heat dissipation balancing in a power converter," in *Proc. IEEE 60th Int. Sci. Conf. on Power and Electrical Engineering of Riga Technical University*, Riga, Latvia, 7-9 Oct. 2019, pp. 1-6, doi: 10.1109/RTUCON48111.2019.8982255

[9] A. Anuchin, F. Briz, I. Gulyaev, A. Zharkov, M. Gulyaeva, and V. Popova, "Heat dissipation balancing in a switched reluctance drive by combined use of active and passive thermal control methods," in *Proc. 20th Int. Symp. on Power Electronics*, Novi Sad, Serbia, 23-26 Oct. 2019, pp. 1-5, doi: 10.1109/PEE.2019.8923285

[10] M. Andresen and M. Liserre, "Impact of active thermal management on power electronics design," *Microelectronics Reliability*, vol. 54, nos. 9-10, pp. 1935-1939, 2014, doi: 10.1016/j.microrel.2014.07.069

[11] B.B. Al-Khamaiseh, M. Razavi, Y.S. Muzychka, and S. Kocabiyik, "Thermal resistance of a 3-D flux channel with nonuniform heat convection in the sink plane," *IEEE Trans. on Components, Packaging and Manufacturing Technology*, vol. 8, no. 5, pp. 830-839, May 2018, doi: 10.1109/TCPMT.2017.2776601

[12] C. Bünnagel, S. Monir, A. Sharp, A. Anuchin, O. Durieux, I. Uria, and Y. Vagapov, "Forced air cooled heat sink with uniformly distributed temperature of power electronic modules," *Applied Thermal Engineering*, vol. 199, Nov. 2021, Art no. 117560, doi: 10.1016/j.applthermaleng.2021.117560

[13] W. Zhao, Z. Ying, X. Song, and R. Xu, "Cost-minimization method for heatsink of multi-parallel power devices considering thermal safety constraints," *Energy Reports*, vol. 7, pp. 306-314, Nov. 2021, doi: 10.1016/j.egyr.2021.10.028

[14] A. Mueller, C. Buennagel, S. Monir, A. Sharp, Y. Vagapov, and A. Anuchin, "Numerical design and optimisation of a novel heatsink using ANSYS steady-state thermal analysis," in *Proc. 27th Int. Workshop on Electric Drives*, Moscow, Russia, 27-30 Jan. 2020, pp. 1-5, doi: 10.1109/IWED48848.2020.9069568

[15] Tecnoal, "I71 heat sink data sheet," [Online]. Available: http://www.tecnoal.it/media/7747/i71.pdf.